ACS OMEGA

http://pubs.acs.org/journal/acsodf

Article

Hydrogel-Mediated Release of TRPV1 Modulators to Fine Tune Osteoclastogenesis

Ranabir Chakraborty, Tusar Kanta Acharya, Nikhil Tiwari, Rakesh Kumar Majhi, Satish Kumar, Luna Goswami, and Chandan Goswami*

Cite This: *ACS Omega* 2022, 7, 9537–9550

Read Online

ACCESS | Metrics & More | Article Recommendations | Supporting Information

ABSTRACT: Bone defects, including bone loss due to increased osteoclast activity, have become a global health-related issue. Osteoclasts attach to the bone matrix and resorb the same, playing a vital role in bone remodeling. Ca^{2+} homeostasis plays a pivotal role in the differentiation and maturation of osteoclasts. In this work, we examined the role of TRPV1, a nonselective cation channel, in osteoclast function and differentiation. We demonstrate that endogenous TRPV1 is functional and causes Ca^{2+} influx upon activation with pharmacological activators [resiniferatoxin (RTX) and capsaicin] at nanomolar concentration, which enhances the generation of osteoclasts, whereas the TRPV1 inhibitor (5′-IRTX) reduces osteoclast differentiation. Activation of TRPV1 upregulates tartrate-resistant acid phosphatase activity and the expression of cathepsin K and calcitonin receptor genes, whereas TRPV1 inhibition reverses this effect. The slow release of capsaicin or RTX at a nanomolar concentration from a polysaccharide-based hydrogel enhances bone marrow macrophage (BMM) differentiation into osteoclasts whereas release of 5′-IRTX, an inhibitor of TRPV1, prevents macrophage fusion and osteoclast formation. We also characterize several subcellular parameters, including reactive oxygen (ROS) and nitrogen (RNS) species in the cytosol, mitochondrial, and lysosomal profiles in BMMs. ROS were found to be unaltered upon TRPV1 modulation. NO, however, had elevated levels upon RTX-mediated TRPV1 activation. Capsaicin altered mitochondrial membrane potential ($\Delta\Psi m$) of BMMs but not 5′-IRTX. Channel modulation had no significant impact on cytosolic pH but significantly altered the pH of lysosomes, making these organelles less acidic. Since BMMs are precursors for osteoclasts, our findings of the cellular physiology of these cells may have broad implications in understanding the role of thermosensitive ion channels in bone formation and functions, and the TRPV1 modulator-releasing hydrogel may have application in bone tissue engineering and other biomedical sectors.

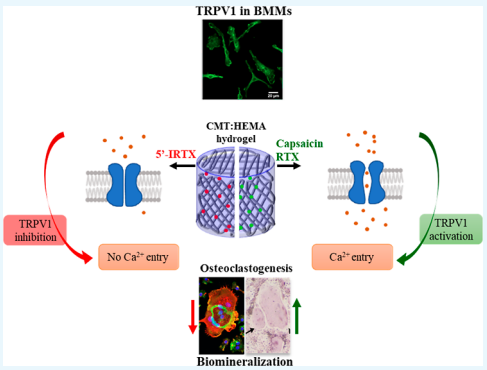

INTRODUCTION

The role of ion channels in the morphological development of organisms is well established, and their functional signaling remains conserved from lower invertebrates to complex mammals. Cation (Na^+, K^+, and Ca^{2+}) channels remain a critical determinant of normal development, alterations in the functions of which have been implicated in several developmental complications, including of the skeletal system.[1] Bones are the major sources of Ca^{2+} in vertebrates, thereby implicating the importance of these ions in skeletal development and maintenance of homeostasis. Deposition or resorption of Ca^{2+} mediates functions of osteoblasts and osteoclasts and thereby strengthening or weakening bones, respectively. Receptor activator of NFκB ligand (RANKL) induces oscillatory changes in intracellular Ca^{2+} concentration of osteoclasts, which regulates their differentiation, maturation, motility, cytoskeletal rearrangements, and bone resorption activity.[2] Intracellular Ca^{2+} homeostasis is regulated by simultaneous release of Ca^{2+} from intracellular stores and/or entry of Ca^{2+} from the extracellular environment. Similarly, Ca^{2+} movement into the intracellular stores and Ca^{2+} pumps reduce the intracellular Ca^{2+} levels.

Transient receptor potential (TRP) channels are a group of nonselective cation channels that are regulated by several endogenous molecules, plant products, and synthetic ligands as well as by environmental cues like pH, stretching, osmolarity, and temperature. Notably, TRPV1 has evolved as a vertebrate-specific protein and its molecular evolution strongly correlates with vertebrate evolution.[3] Accordingly, regulation of musculoskeletal development by members of the TRP superfamily of nonselective cation channels has been demonstrated by skeletal deformities caused by disrupting mutations of TRPV4.[4] Among other members of the TRPV family, the TRPV5 and TRPV6

Received: December 7, 2021
Accepted: February 1, 2022
Published: March 9, 2022

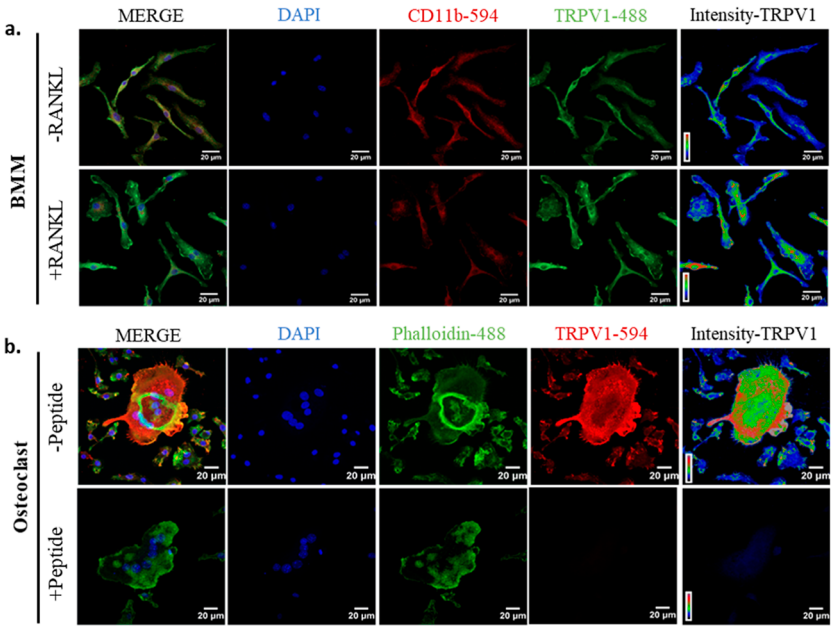

Figure 1. Expression and functional analysis of TRPV1 in BMMs and Osteoclasts. (a) BMMs stained for the macrophage marker CD11b (red) and TRPV1 (green) depict the latter's expression in these cells, both in the absence (upper panel) and presence (lower panel) of RANKL. (b) Expression of TRPV1 (red) in phalloidin-stained osteoclasts (green, upper panel) is confirmed by a peptide segment against anti-TRPV1 antibody (lower panel) that reduces the specific fluorescence signal intensity of the TRPV1 channel.

channels are highly Ca^{2+}-selective and have been implicated in regulating Ca^{2+} dynamics and bone reabsorption activity of osteoclasts.[5] TRPV2 and TRPV4 channels have also been implicated in RANKL-mediated oscillations, osteoclast differentiation, and functions.[6] TRPV1 (also known as the "capsaicin receptor") has high Ca^{2+} permeability and is present in neuronal and non-neuronal cells.[7] Genetic deletion of TRPV1 inhibits osteoclast formation and differentiation in $TRPV1^{-/-}$ mice.[8] This is supported by another observation that TRPV1 antagonist capsazepine inhibits osteoclast differentiation *in vitro* and ovariectomy-induced bone loss *in vivo*.[9]

These findings prompted us to investigate the endogenous expression of TRPV1 in osteogenic cells and if pharmacological modulation of TRPV1 affects osteoclastogenesis. Thus, in this work, we pharmacologically activate and inhibit TRPV1 to characterize its role in differentiating osteoclasts *in vitro*. We have developed a hydrogel-based drug delivery system for the slow release of TRPV1 modulators and show that this *in vitro* condition is highly efficient in enhancing osteoclast differentiation. The hydrogel-coated delivery of TRPV1 modulators offers effective tools to control bone marrow macrophages (BMMs) at the cellular (structural) and subcellular (functional) levels.

RESULTS

The interplay between osteoblasts and osteoclasts is critical in maintaining bone homeostasis. In both *in vitro* and *in vivo* conditions, osteoblasts promote the differentiation of hematopoietic stem cells into macrophages via the macrophage colony-stimulating factor (MCSF)-driven paracrine signaling.[10] The local microenvironment of bone induces the formation of osteoclasts from BMMs via RANKL secreted by osteoblasts, osteocytes, and chondrocytes.[11] Abnormal activity of osteoclasts has been shown to cause osteosclerotic bone defects, such as osteoporosis (excessive activity of osteoclasts).[12]

Endogenous TRPV1 Expression in BMMs and Osteoclasts. To check for the presence of TRPV1, we performed immunofluorescence staining of both BMMs and differentiated osteoclasts. In both cases, we observed endogenous expression of TRPV1 in these cells (Figure 1a,b). The expression has a marginal increase in mononucleated macrophages in the presence of RANKL (for 2 days) (Figure 1a, lower panel). A longer treatment of BMMs with RANKL (8 days) results in the formation of multinucleated osteoclasts, which show higher TRPV1 intensity relative to the neighboring mononucleated BMMs (Figure 1b, upper panel). In osteoclasts, TRPV1 intensity was higher at the periphery and podosomes, whereas it was scarce at the adhesion zone (also known as "sealing zone") formed by the actin ring (stained by Phalloidin-488), a characteristic feature of osteoclasts. The fidelity of TRPV1 detection is confirmed by using a peptide blocker against the primary antibody, wherein TRPV1 remains undetected (Figure 1b, lower panel).

TRPV1 is Functional and Allows Ca^{2+} Influx in BMMs. The functionality of an ion channel was determined by its ability to allow the movement of ions through it. Given the high conductance probability of TRPV1 channels towards Ca^{2+}, we assessed their functional status by performing live-cell imaging using the Ca^{2+}-sensitive dye Fluo4-AM that allows for detection of the intracellular Ca^{2+} level. Both capsaicin (10 nM) and resiniferatoxin (RTX, 10 nM) induced TRPV1 activation-mediated elevation in the intracellular Ca^{2+} level in BMMs, a response which eventually decayed as the cell restored the homeostatic level of the ion (Figure 2a–c). Inhibition of TRPV1 using 5′-iodoresiniferatoxin (5′-IRTX, 1 μM) did not elevate intracellular Ca^{2+} levels. Using another Ca^{2+}-sensitive dye, Rhod3-AM, the application of RTX (10 nM) increases the intracellular level of the ions in BMMs (Figure S1a). Taken together, these data are suggestive of a functional TRPV1 in BMMs.

https://doi.org/10.1021/acsomega.1c06915
ACS Omega 2022, 7, 9537−9550

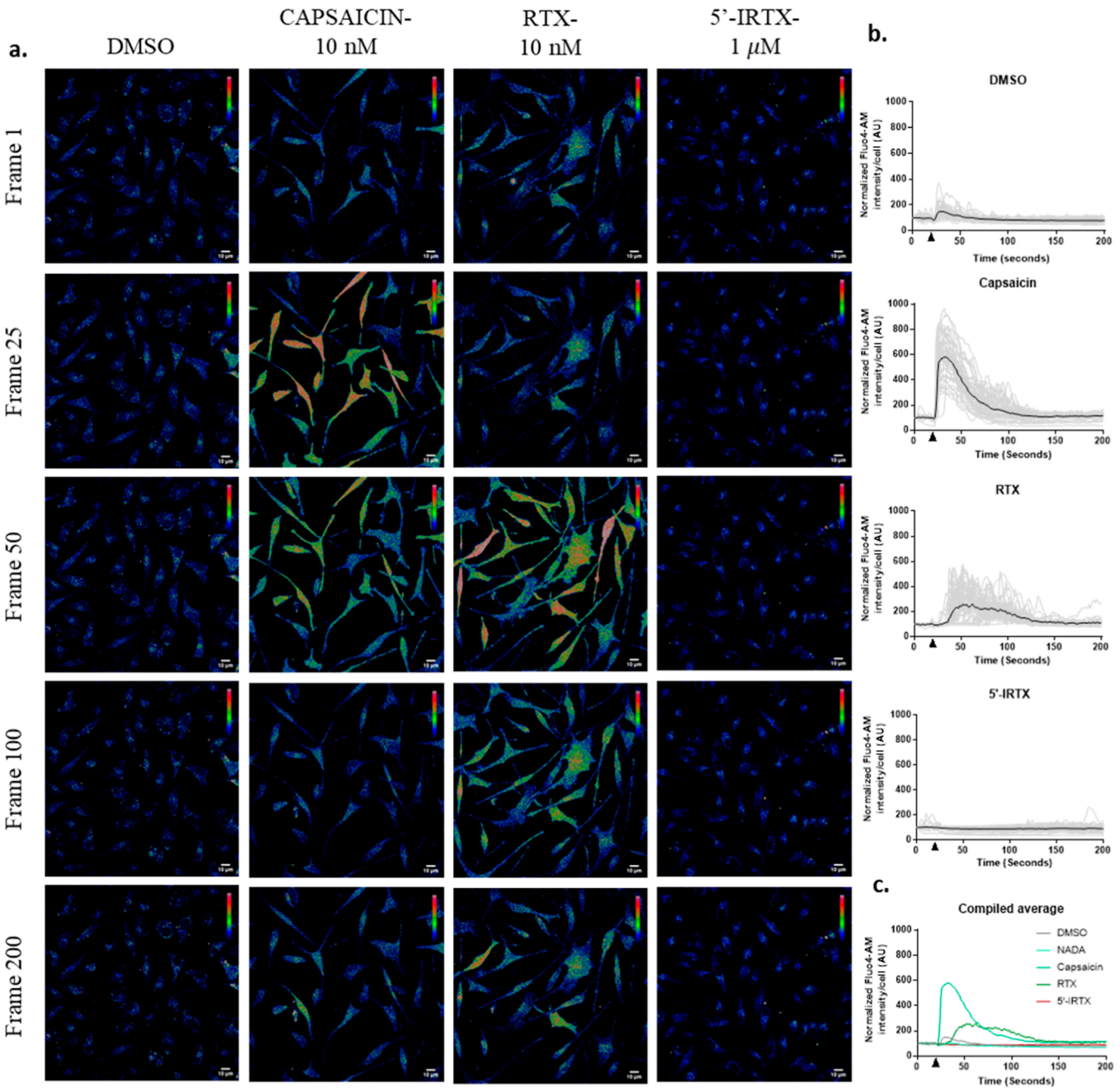

Figure 2. Functional analysis of TRPV1 in BMMs. (a) BMMs were assessed for intracellular Ca^{2+} levels upon TRPV1 modulation. Representative intensity profiles of Fluo4-AM intensity at different frames are indicated. (b) Time series graphs of intracellular Fluo4-AM intensities across 200 frames of live imaging. The arrow at the x-axis signifies the time of addition of the respective drugs (20th frame). Gray traces are of individual cells, and the black trace represents the average of 50 cells. (c) Compiled average of different treatments of BMMs, individual cell traces omitted.

TRPV1 Regulates Differentiation of BMMs. The presence of functional TRPV1 in BMMs prompted us to investigate its potential role in the context of differentiation of these cells to osteoclasts. The differentiation assay was performed by performing a tartrate-resistant acid phosphatase (TRAP) assay. TRAP is an osteoclast-specific marker which gives brown-red coloration upon staining. Co-application of RANKL with TRPV1-specific agonist RTX (1 nM) resulted in an increased number of TRAP-positive, multinucleated cells (Figure S2a−c) as compared to cells not activated for TRPV1 (only MCSF, and MCSF + RANKL). The addition of TRPV1 inhibitor (5′-IRTX, 10 μM) prevented differentiation of BMMs into osteoclasts, despite the presence of the osteoclastogenesis stimulator RANKL (Figure S2a−c). Under this condition, all the cells remained as mononucleated BMMs. Taken together, these results suggest that TRPV1 plays an active role in the differentiation of BMMs, as blocking TRPV1 activity prevents the process in its precursor stage.

TRPV1 Regulates Expression of Osteoclast-Specific Genes. To assess the molecular changes happening as a function of TRPV1 activation in the process of osteoclastogenesis, we performed quantitative determination of mRNA levels of two osteoclast markers, cathepsin K (CTK) and calcitonin receptor (CTR), using glyceraldehyde-3-phosphate dehydrogenase (GAPDH) as the housekeeping gene control. RTX (1 nM) increases the level of both CTK and CTR in

https://doi.org/10.1021/acsomega.1c06915
ACS Omega 2022, 7, 9537−9550

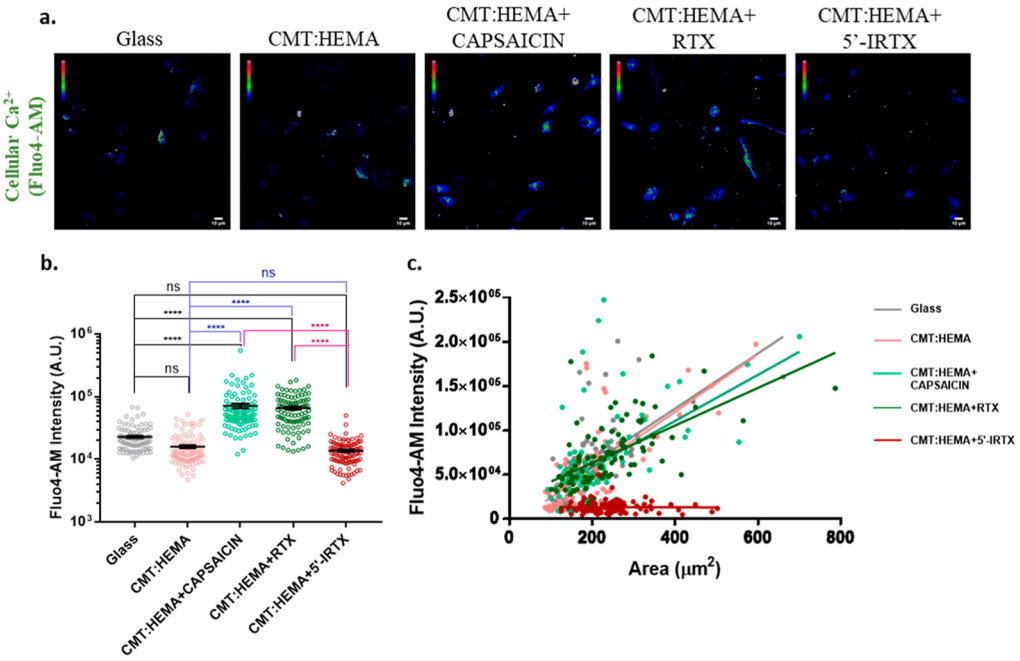

Figure 3. Functional analysis of TRPV1 in BMMs grown on the CMT:HEMA hydrogel. (a) BMMs grown on hydrogels to check for the endogenous levels of Ca^{2+} using Fluo4-AM Ca^{2+}-sensitive dye. TRPV1 activation elevates the intracellular Ca^{2+} levels, as is quantified in (b); $n = 100$ cells; one-way ANOVA; ns: non-significant, ****$p < 0.0001$. (c) Correlation representation of the area of cells and per unit area intensity of Fluo4-AM depicts strong positive correlations under basal and TRPV1-activated conditions but not upon inhibition of the channel.

differentiating BMMs significantly, whereas 5′-IRTX (10 μM) almost completely blocks generation of these transcripts (Figure S2d,e). TRPV1 activation thereby brings about changes at a transcript level in BMMs to regulate the formation of osteoclasts.

Utilization of the CMT:HEMA Hydrogel for Bone Tissue Engineering. The three-dimensional scaffold of bones ensures efficient bone remodeling *in vivo* upon injury. With advancements in biomaterials, recapitulating such a phenomenon *in vitro* has garnered significant interest in current times. We have previously introduced a novel polysaccharide-based hydrogel CMT:HEMA[13] as an effective matrix for skin[14] and bone[15] tissue engineering. In order to deliver TRPV1 modulators in a controlled manner, we chose to encapsulate TRPV1 modulators in CMT:HEMA, which can get degraded over time and ensure slow release of drugs encapsulated within it. The surface microstructure of the hydrogel revealed a highly interconnected, porous matrix that allows for cells to efficiently attach and proliferate.[15]

***In Vitro* Sustained Release of Capsaicin from the CMT:HEMA Hydrogel.** A major route of pharmaceutical drug administration (oral) is limited by nonspecific targeting, short half-lives, and reduced circulation time.[16] Systemic metabolic degradation of the molecules also remains a hurdle in generating the desired physiological response efficiently. To overcome these issues, recent research has focused on sustained and controlled drug delivery systems using novel devices such as nanoparticles, liposomes, hydrogels, and so forth.[17] Hydrogel-based drug delivery systems can manage the availability of drug to cells and tissues over space and time. These result in the enhancement of their therapeutic efficacy and reduction in their cytotoxicity and requisite dosage. To analyze the release property of the CMT:HEMA hydrogel, we tested the release kinetics of capsaicin. Initially, a sharp burst release of the drug was observed within 2 h, which may be due to the release of a surface- absorbed drug and initial rapid swelling of the hydrogel. Eventually, a slow, sustained, and stable drug release profile was observed for up to 16 h, after which a plateau stage was reached. Approximately 74% capsaicin was released within 23 h (data not shown). These observations stipulate the potential of the CMT:HEMA hydrogel as a sustained drug delivery system which can be used as a drug delivery agent *in vivo*.

Drug-Infused Hydrogels Efficiently Modulate TRPV1 Function. To evaluate the response of TRPV1 in the presence of its activators and inhibitor infused in the hydrogel, endogenous Ca^{2+} levels were measured using Fluo4-AM. Cells grown on hydrogels with TRPV1 activators (capsaicin, 1 nM, and RTX, 1 nM) show significantly higher intracellular Ca^{2+} levels relative to cells grown with (CMT:HEMA only) or without (glass) the hydrogel (Figure 3a,b). The inhibitor 5′-IRTX-infused hydrogel did not elevate the Ca^{2+} level in cells grown on it. Taken together, these results suggest the functional efficacy of the drug-infused hydrogel as a potent modulator of TRPV1 activity. The extent of endogenous levels of Ca^{2+} is positively correlated with statistical significance to the area of the cells under all experimental conditions but not in the presence of the TRPV1 inhibitor 5′-IRTX (Figures 3c, S1b).

Morphometric Analyses of Cells Grown on Hydrogels. In order to assess the influence of the hydrogel (with and without TRPV1 modulators) on morphology of cells, we stained for F-actin in BMMs in the presence of RANKL (Figure 4a). The intensity of phalloidin per unit area of cells decreased significantly when grown on hydrogels compared to those grown on glass (Figure 4b). Additionally, the presence of TRPV1 activators did not affect F-actin levels in comparison to the CMT:HEMA control, which itself had significantly reduced F-actin levels as compared to cells grown on glass. This prompted us to check for the reason behind the observed differences. Morphometric analyses indicate no significant changes in both the area and perimeter of cells when grown in

https://doi.org/10.1021/acsomega.1c06915
ACS Omega 2022, 7, 9537−9550

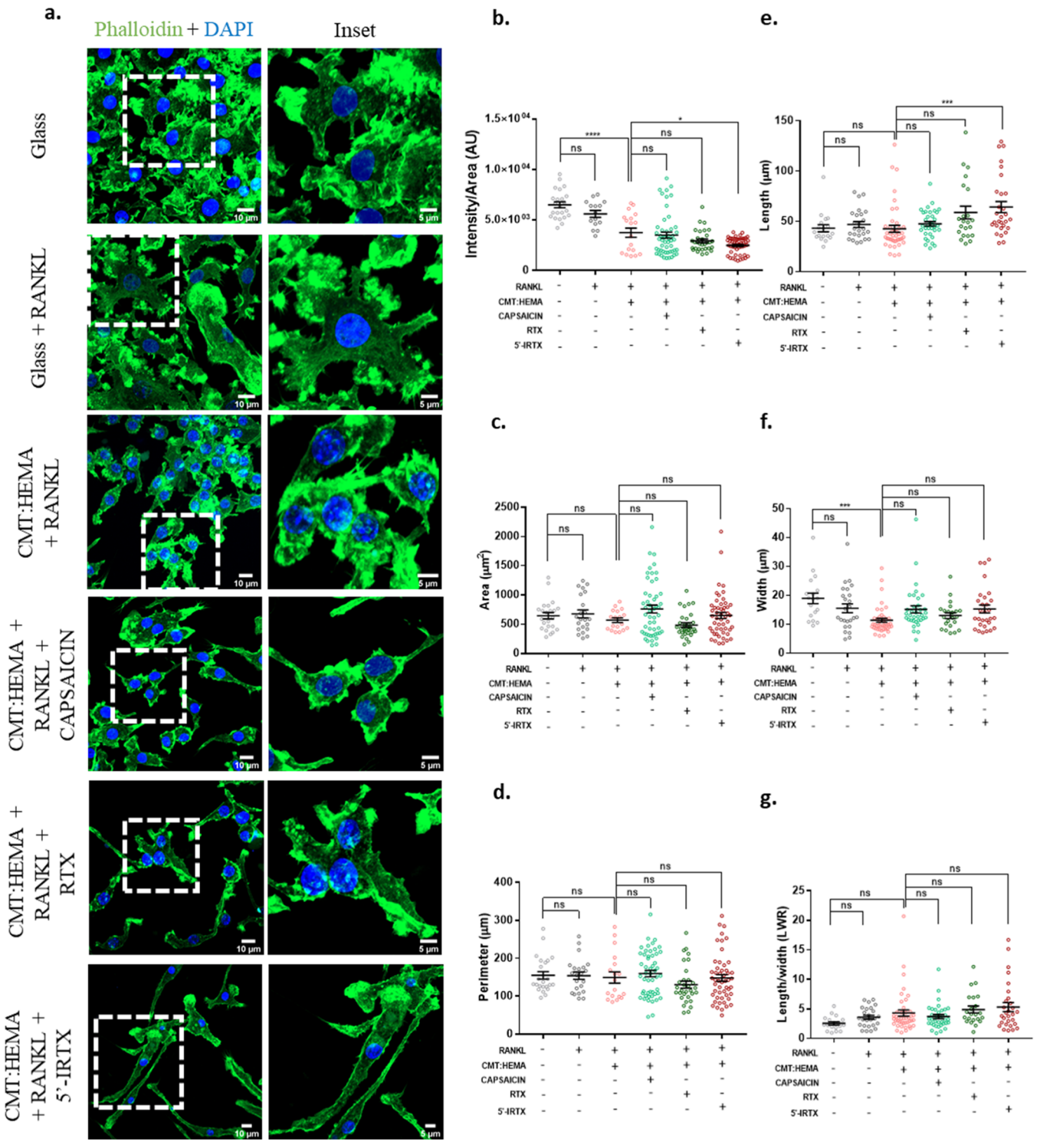

Figure 4. Morphological analysis of BMMs grown on the hydrogel. (a) Representative images of BMMs grown on glass or hydrogel in the presence of RANKL and TRPV1 modulators. Right panels denote marked inset of respective images. Phalloidin intensity (b) and morphometric analyses of BMM's area (c), perimeter (d), length (e), width (f), and LWR (g). $n = 18-51$ cells per group; one-way ANOVA; ns: non-significant, $^{*}p < 0.05$, $^{***}p < 0.001$, $^{****}p < 0.0001$.

the presence of TRPV1 activators and inhibitor (Figure 4c,d). The presence of hydrogel (CMT:HEMA + RANKL) reduces the width of BMMs grown on it without affecting the length, which, however, is increased in the presence of 5′-IRTX (Figure 4e,f), thereby contributing to the lowered F-actin intensity distribution in these cells. The length−width ratio (LWR) remains unchanged under the conditions analyzed (Figure 4g). These structural variations could be an initiation event in the modulation of differentiation and migration abilities of BMMs.

CMT:HEMA Encapsulating TRPV1 Modulators Does Not Influence Cytosolic ROS of BMMs. Reactive oxygen species (ROS) are produced during aerobic respiration in the electron transport chain and have been implicated in regulating several cellular functions. ROS have been reported to act as

https://doi.org/10.1021/acsomega.1c06915
ACS Omega 2022, 7, 9537−9550

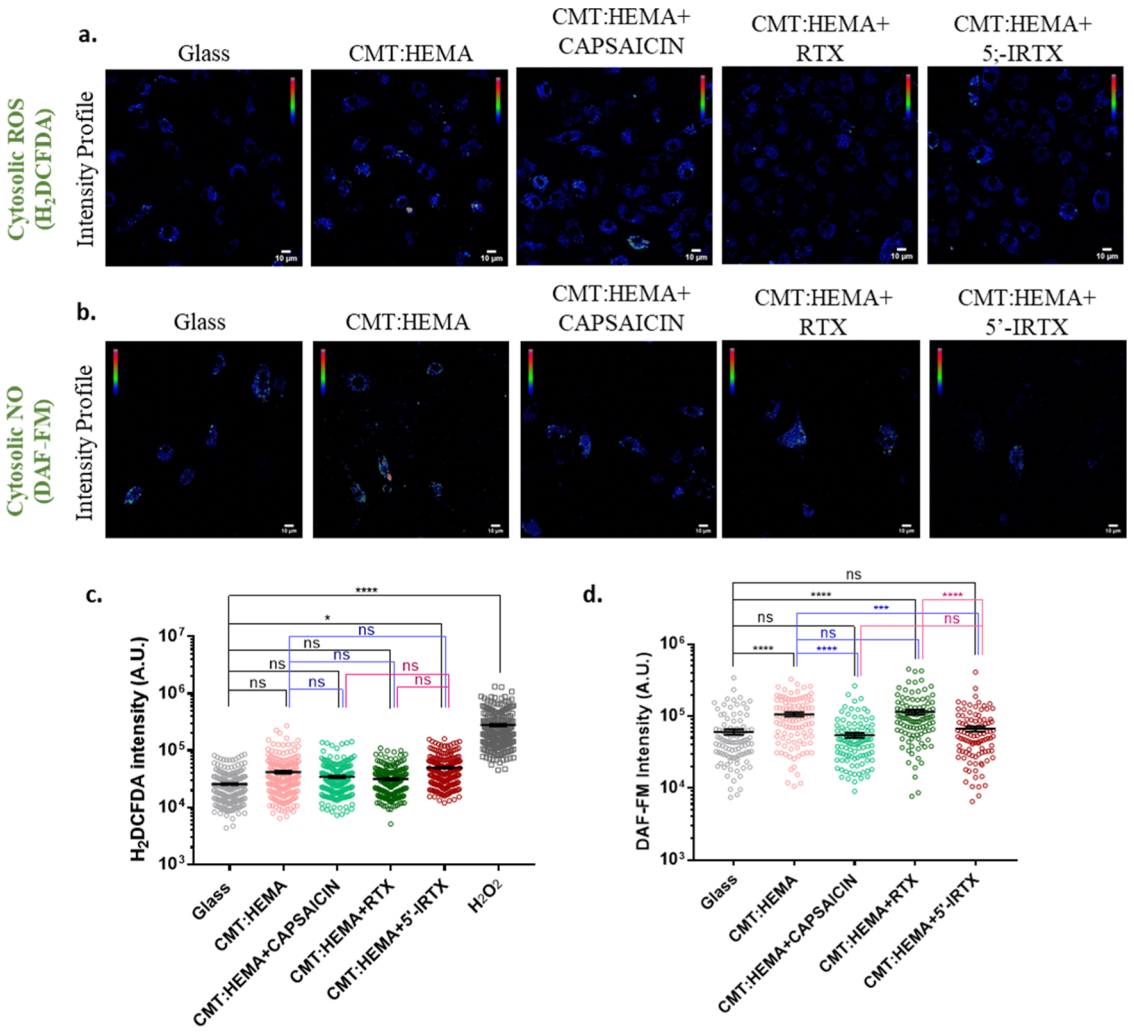

Figure 5. Subcellular parameters (cytosolic ROS and NO) of BMMs grown on the hydrogel. (a,c) Intensity profiles of ROS (H_2DCFDA staining) and its quantitation. n = 250 cells per group; one-way ANOVA. (b,d) Intensity profiles of NO (DAF-FM staining) and its quantitation. n = 100 cells per group; one-way ANOVA; ns: non-significant, *$p < 0.05$, ***$p < 0.001$, ****$p < 0.0001$.

secondary messengers regulating gene expression and regulation of downstream signaling events, allowing for cell survival, proliferation, differentiation, migration, and apoptosis.[18] ROS signaling also plays an important role in maintenance of bone homeostasis by functioning as a positive regulator of osteoclastogenesis.[19] Besides the beneficial roles of ROS at a physiological level, these have also proven to be detrimental to cells by directly affecting lipids, proteins, and nucleic acids.[20] This prompted us to check for cytosolic superoxide species in BMMs before the induction of differentiation. When grown on hydrogels, TRPV1 activators capsaicin and RTX and the inhibitor 5′-IRTX had comparable intracellular ROS levels to the CMT:HEMA hydrogel control (Figure 5a,c). The CMT:HEMA hydrogel itself did not have a significant impact on cytosolic ROS as compared to control cells grown on glass.

TRPV1 Regulates Cytosolic NO Production. Reactive nitrogen species (RNS) have been shown to regulate osteoclast functions.[21] We assessed for the RNS nitric oxide (NO) in BMMs grown on hydrogels. Although TRPV1 activation by capsaicin did not have any effect on the NO level compared to cells grown on glass, activation by RTX significantly increased cytosolic NO (Figure 5b,d), suggestive of the differential impact generated by the two compounds as has been previously reported (Kumar et al., 2013). In contrast, TRPV1 inhibition did not elevate NO levels.

TRPV1 Modulates Mitochondrial Membrane Potential and Cardiolipin Level. We checked for the indicators of mitochondrial health as readouts of cardiolipin levels, an integral phospholipid of the inner mitochondrial membrane and organellar membrane potential. Using 10-*N*-nonyl-acridine orange (NAO), capsaicin-mediated TRPV1 activation was found to compromise mitochondrial health as observed by reduced cardiolipin signal intensity per cell (Figure 6a,c). Both RTX and 5′-IRTX, on the other hand, had an apparent positive impact on mitochondria. Measurement of mitochondrial membrane potential by the ratiometric indicator JC-1 also shows a TRPV1 activation-dependent decrease in mitochondrial potential (Figure 6b,d), while inhibition of TRPV1 did not have any negative effect. Taken together, hydrogel-mediated long-term pharmacological activation of TRPV1 affects mitochondrial functions.

TRPV1 Modulates Cytosolic and Lysosomal pH. We next checked for any changes in pH of the cytosol and lysosomes of hydrogel-grown BMMs. Using pHrodo, a cytosolic pH indicator, capsaicin, but neither RTX nor 5′-IRTX, was observed to elicit an acidification response (Figure 7a,b). The lysosomal

https://doi.org/10.1021/acsomega.1c06915
ACS Omega 2022, 7, 9537−9550

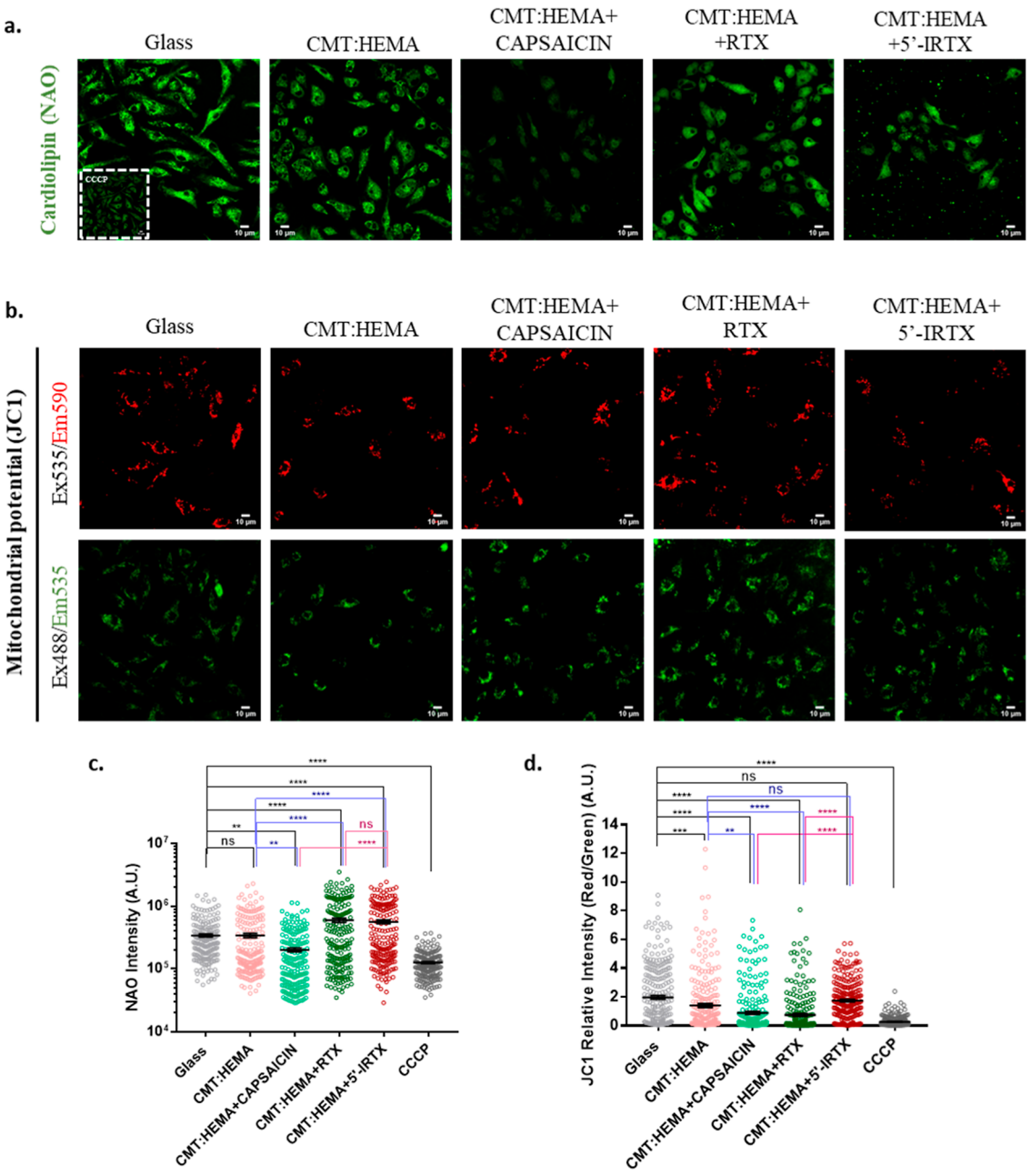

Figure 6. Mitochondrial profiles of BMMs grown on the hydrogel. (a,c) Representative images of cardiolipin (NAO staining) and its quantitation. n = 200 cells per group; one-way ANOVA. (b,d) Mitochondrial membrane potential as measured by the ratiometric dye JC-1 and its quantitation. n = 250 cells per group; one-way ANOVA; ns: non-significant, $^{**}p < 0.01$, $^{***}p < 0.001$, $^{****}p < 0.0001$.

profile in BMMs was assessed by LysoTracker red. Whole-cell intensity of the dye suggests an increase in abundance of viable lysosomes in the presence of RTX and 5′-IRTX (Figure S3a,b). Capsaicin, however, had an opposite effect, wherein the reduced fluorophore intensity could be suggestive of a change in either lysosomal number or their pH. Validation of the same using LysoSensor green suggested an increase in lysosomal pH (become less acidic) in the case of capsaicin, an effect that was also observed to an even greater extent in the presence of RTX and 5′-IRTX (Figure 7c,d). Taken together, these results suggest a fine control of both cytosolic and lysosomal pH in the presence of TRPV1 modulators.

Hydrogel Releasing TRPV1 Modulators Efficiently Regulates Osteoclast Formation. BMMs were grown on drug-infused hydrogels and assessed for their differentiation potential. The presence of RTX (1 nM) significantly increased the propensity of BMMs to differentiate (Figure 8a,c) as observed by the increase in TRAP-positive, multinucleated cells. 5′-IRTX, however, did not induce any osteoclast formation. Activation of TRPV1 by capsaicin (1 nM) also significantly upregulated osteoclast formation (Figure 8b). In comparison to the control (only RANKL), the presence of both capsaicin and RTX was able to increase osteoclastogenesis by ∼20% (Figure 8a−c). Interestingly, even a low concentration of both these activators initiates the BMM differentiation response. These results not only suggest the importance of TRPV1 modulation in osteoclastogenesis but also highlight the potency of the hydrogel used in efficiently delivering nanomolar concentration of drugs for generating a response.

https://doi.org/10.1021/acsomega.1c06915
ACS Omega 2022, 7, 9537−9550

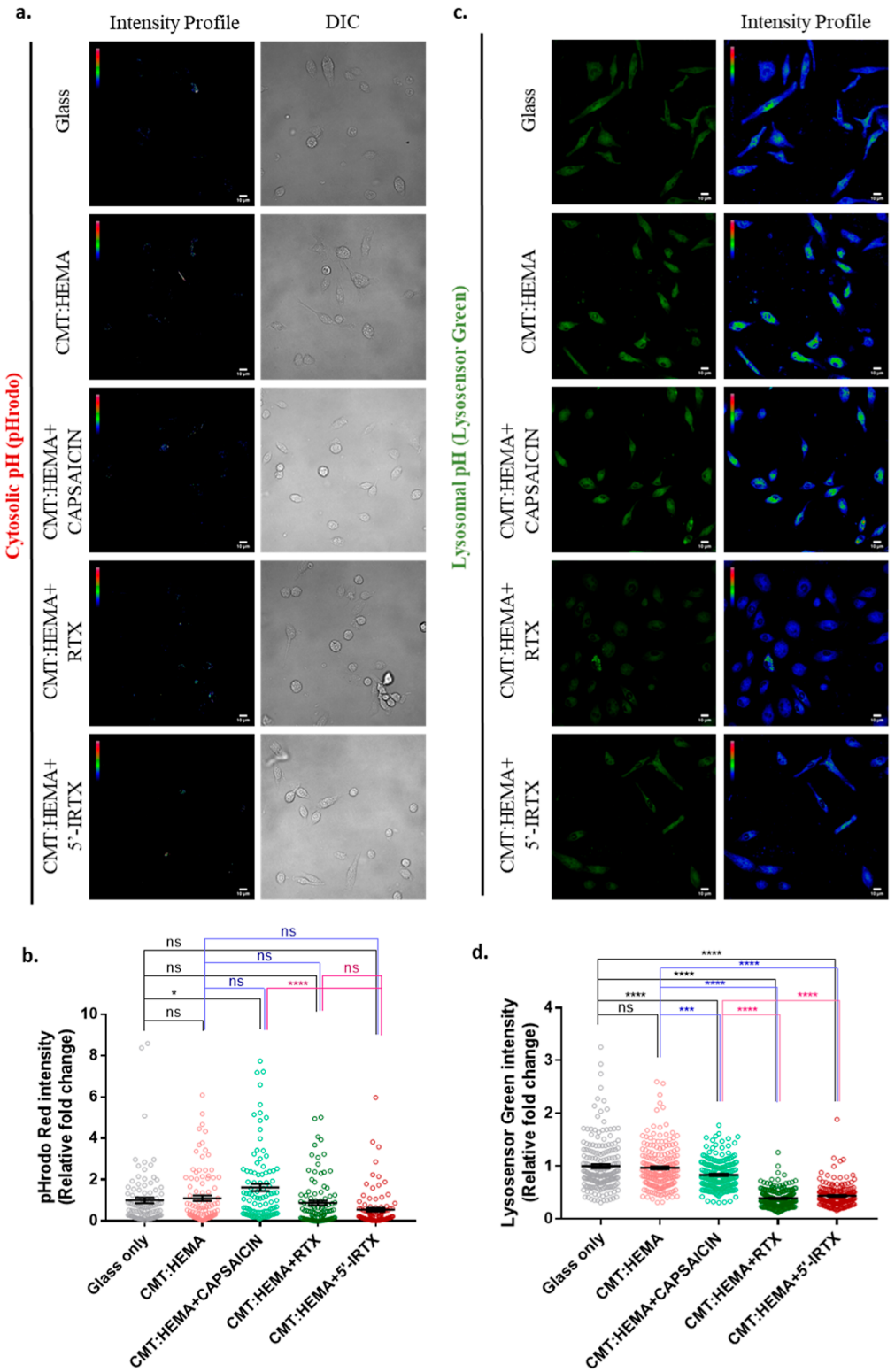

Figure 7. Cytosolic and lysosomal pH of BMMs grown on the hydrogel. (a,b) Intensity profiles of cytosolic pH (a; left vertical panels) with the corresponding DIC images (a; right vertical panels) and their quantitation. (c,d) Lysosomal pH as measured using the pH-sensitive dye LysoSensor green (c; left vertical panels) with their corresponding intensity profiles (c; right vertical panels) and their quantitation. n = 200 cells per group; one-way ANOVA; ns: non-significant, $^{**}p < 0.01$, $^{***}p < 0.001$, $^{****}p < 0.0001$.

DISCUSSION

Bone is a rigid yet dynamic connective structure in the body. It needs to have the proper microarchitecture to ensure that it provides maximum strength with minimal mass.[22] As such, bone is constantly remodeled by the synthesis of new bone material by osteoblast differentiation and mineralization and resorption by osteoclasts. Bone homeostasis depends on proper coordination between osteoblasts and osteoclasts. While osteoclast differentiation and maturation depend on MCSF and RANKL

https://doi.org/10.1021/acsomega.1c06915
ACS Omega 2022, 7, 9537−9550

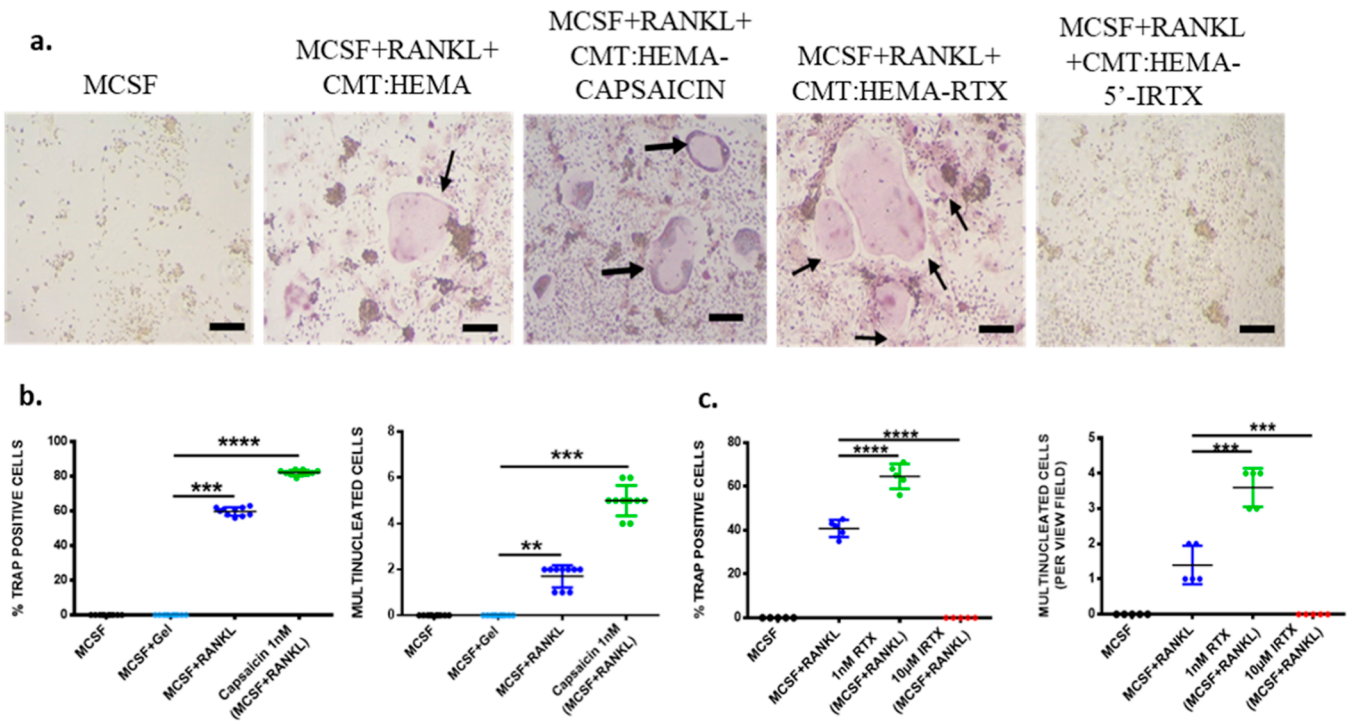

Figure 8. Differentiation propensities of BMMs into osteoclasts grown on hydrogel. (a) Representative TRAP assay of BMMs grown on the hydrogel in the presence of the TRPV1 activator (RTX) and inhibitor (5′-IRTX) under differentiating conditions (MCSF + RANKL). (b,c) Quantitation of TRAP-positive cells and multinucleated cells in the presence of capsaicin (b) and RTX (c) shows elevated osteoclastogenesis as compared to MCSF and CMT:HEMA control groups. $n = 5-10$; one-way ANOVA; $^{**}p < 0.01$, $^{***}p < 0.005$, $^{****}p < 0.001$.

secreted by osteoblasts, osteoclasts in turn secrete certain factors like BMP6 and Wnt10b that promote osteoblast recruitment and maturation, thereby promoting bone formation.[23] The process of differentiation of BMMs into osteoclasts is tightly regulated by Ca^{2+} signaling. RANKL binds to its receptor RANK present on preosteoclasts (BMMs), which then recruits adaptor molecules including TRAF6. TRAF6 subsequently activates NFκB, which induces production of the transcription factor NFATc1, the master regulator that activates transcription of osteoclast-specific genes.[24] Maturation of osteoclasts results in the formation of an "adhesion zone", formed by a filamentous actin ring (also known as "sealing zone"), which helps in adhering to the bone. Osteoclasts initially demineralize the bone by dissolving its calcium phosphate crystals and then degrade the exposed extracellular matrix (resorption), causing bone decay.[25] Such bone decay is a serious medical problem in different patient groups and in aged women after menopause.[26] The involvement of TRP ion channels in regulation of bone homeostasis has been well established. Deletion of TRPV1 in mice leads to impairments in osteoclastogenesis and fracture healing.[8] Reduced osteoclastogenesis due to TRPV1 KO consequently results in increased bone mass.[27] In conditions involving low bone density, increased osteoclast activities have been shown to be a driving force, which can be rescued upon inhibition of TRPV1, thereby suggesting a pharmacologically active premise of bone remodeling via TRPV1 regulation.[28]

In this study, we found that endogenous TRPV1 expression in BMM increases upon stimulation with RANKL for 3 days, indicating that TRPV1 is upregulated during differentiation of BMMs. The expression level of TRPV1 is much higher in mature osteoclasts, which could correlate with its functional role in differentiation and maturation of osteoclasts. Interestingly, TRPV1 is primarily enriched in the cell membrane region, indicating that much of the intracellular Ca^{2+} rise upon TRPV1 activation by RTX can be primarily due to the entry of Ca^{2+} ions from the extracellular environment. This also matches well with the function of osteoclasts as major Ca^{2+}-reabsorbing cells. The differentiating BMMs fuse to form multinucleated osteoclasts. These mature osteoclasts actively synthesize lysosomal enzymes, in particular, TRAP (used as a marker of the osteoclasts) and cysteine proteinases such as the cathepsins. TRPV1 activation is able to enhance RANKL-mediated differentiation of BMMs into osteoclasts, whereas TRPV1 inhibition prevents RANKL-mediated osteoclast formation. This indicated that although TRPV1 activation itself is not able to induce osteoclastogenesis, it provides a synergistic effect to the RANKL-mediated signaling event. Notably, the results suggest that TRPV1 function is essential for RANKL-mediated osteoclastogenesis. This is in full agreement with previous reports that have shown that TRPV1 knockout mice have reduced osteoclast formation[8] and that TRPV1 inhibition prevents osteoclast formation and increase in bone loss that is expected to occur in ovariectomized mice.[9] Quantitative determination of mRNA levels of two osteoclast markers, CTK and CTR revealed that TRPV1 affects the downstream signaling mechanism involved in osteoclastogenesis. Previously, it has been shown that mice fed with plant products activating TRPV1, namely gingerol or capsaicin, have a higher degree of trabecular osteoclast formation, eroded microarchitecture of trabecular bone, and reduced vertebral bone density, which was comparable to those of ovariectomized mice.[29]

The relevance of understanding physiological states of osteoclast precursor cells (BMMs) remains of great interest in modulating osteoclast formation and integration into the bone cytoarchitecture. Based on our previous reports of the CMT:HEMA hydrogel acting as a reliable matrix for bone

https://doi.org/10.1021/acsomega.1c06915
ACS Omega 2022, 7, 9537−9550

tissue engineering,[15] we characterized several cellular and subcellular parameters of BMMs grown on this hydrogel in the presence and absence of TRPV1 pharmacological modulators. Although the hydrogel did not have an impact on the area and perimeter of BMMs, the length and breadth of these cells elicited differences under certain conditions. The presence of the hydrogel was sufficient to reduce the width of cells but not their length. This is suggestive of attainment of a compact morphology owing to the porous, highly interconnected ultrastructure of the hydrogel scaffold. Inhibition of TRPV1 significantly increases the length of BMMs, thereby indicating a possible impairment in the formation of cellular clusters for efficient osteoclastogenesis. TRPV1 activators also show reduced actin levels and increased proximity, facilitating their fusion to form multinucleated osteoclasts. This process can possibly be mediated by the intracellular Ca^{2+} level, which is diminished upon TRPV1 inhibition. A decline in the basal level of cytosolic Ca^{2+} potentially reduces the probability of such events. 5′-IRTX-mediated reduction in intracellular Ca^{2+} is accompanied by a negative correlation of Fluo4-AM intensity with the area of the cell, suggesting a decoupling of area-dependent endogenous Ca^{2+} levels increase and subsequent accumulation upon TRPV1 inhibition.

The levels of superoxide species in cells were not significantly altered in the presence of TRPV1 activators. Since the ROS levels were measured after 24 h in culture, the differences in our results from published literature[30] could be attributed to a long-term effect of TRPV1 modulation, possibly allowing for homeostatic maintenance. As such, the use of this hydrogel-based drug delivery system does not have a negative impact on the health of cells via ROS signaling. NO has been reported to negatively regulate the process of osteoclastogenesis both *in vitro* and *in vivo* in an autocrine negative feedback mechanism.[31] In agreement with this, BMMs grown on capsaicin-infused hydrogel have a lowered level of NO as compared to the CMT:HEMA control, thereby indicating the physiological preparation of BMMs to form osteoclasts. Although RTX and 5′-IRTX did not have the expected influence on NO level corroborating the existing results, the absence of RANKL under experimental conditions allows us to highlight the physiology of precursor cells before a differentiating condition is established. Notably, there are certain differences in terms of responses observed in capsaicin-treated and RTX-treated groups (given both are TRPV1 activators). Such differences can arise from a multitude of reasons pertaining to the chemical and pharmacological characteristics of these two compounds. Capsaicin and RTX have different molecular structures and have different solubility in water and oil. Capsaicin is relatively more hydrophobic than RTX, and hence different cell membrane permeabilities. Capsaicin is also known to induce membrane damage. Both have different binding pockets on the TRPV1 channel. Therefore, the optimum concentrations required for activation of TRPV1 are also different.

The role of Ca^{2+} in the maintenance of mitochondrial structure and functions is well established. Osteoclastogenesis has high energy and metabolic requirements. Mature osteoclasts have increased numbers of mitochondria that are not only bigger in size but also have greater interconnectivity among themselves.[32] Therefore, we asked if the mitochondrial profiles are altered in osteoclast precursors upon TRPV1 modulation. Being an integral component of the inner mitochondrial membrane, cardiolipin is an indicator of mitochondrial health. In unhealthy mitochondria, the level of cardiolipin reduces and hence becomes a reliable indicator of the same. Chronic activation of TRPV1 by capsaicin, but not RTX, reduces cardiolipin levels. This difference between the two agonists may be due to their relative hydrophobicity, and there are several cases where capsaicin and RTX differ in terms of TRPV1-mediated cellular effects.[33] In contrast, 5′-IRTX does not induce any such changes. Since our experiments were carried out in the absence of RANKL, these results are indicative of a possible differential regulatory mechanism of maintenance of mitochondrial functions in BMMs in comparison to osteoclasts, wherein TRPV1 modulation can bring about different responses. Corroborating these findings, the mitochondrial membrane potential-based analysis of organellar health also indicates the same line of thought, as both capsaicin and RTX but not 5′-IRTX have detrimental effects on mitochondrial potential.

Although TRPV channels are primarily detected in the plasma membrane and in the endoplasmic reticulum (ER), in recent times, TRPV members have been detected in subcellular organelles such as in mitochondria and in lysosome.[34] Therefore, it is possible that these channels present in different subcellular organelles contribute to the maintenance of Ca^{2+} and pH, not only for the cytosol but also for these organelles. The activity of osteoclasts is highly dependent on functional lysosomes. Osteoclasts form resorption lacunae, a low-pH−high-protease zone, which allows for efficient resorption of bone extracellular matrix.[35] Changes in cytosolic pH have been shown to regulate several intracellular processes including buffering of Ca^{2+} ions to maintain homeostasis.[36] Elevation of intracellular Ca^{2+} concentration in neurons during action potential results in a decrease of intracellular pH caused due to the exchange of Ca^{2+} for H^+ via Ca^{2+}/H^+ pumps.[37] In macrophages, acidification of the cytosol has been shown to cause a rise in the intracellular Ca^{2+} level, thereby suggesting a strong relationship between the two.[38] In addition, TRPV1 has been shown to be present on the ER membrane, which acts as a store of Ca^{2+} in cells.[39] Consequently, we assessed for lysosomal function using LysoSensor green, and cytosolic pH using pHrodo. Cytosolic pH becomes significantly acidic in the presence of capsaicin but not RTX or 5′-IRTX. Lysosomal pH, on the other hand, had a tendency to reach a less acidic value upon TRPV1 modulation, as compared to cells grown either on glass or only on the hydrogel. The presence of capsaicin, however, has a lesser impact on deacidification of lysosomes but not RTX and 5′-IRTX. Since these experiments were performed in the absence of RANKL, the results are indicative of the precursor physiological states of BMMs, which remain amenable to change upon induction of osteoclastogenesis.

In this work, we demonstrate that the capsaicin-encapsulated CMT:HEMA hydrogel has an impact on BMM functions toward osteoclastogenesis. This hydrogel degrades slowly and releases capsaicin slowly. The CMT:HEMA hydrogel by itself does not have any osteoclastogenic potential. However, the capsaicin- and RTX-releasing hydrogels enhance osteoclasts formation from BMMs, while the 5′-IRTX-releasing hydrogel completely inhibits osteoclast formation. This indicates that the hydrogel encapsulating TRPV1 modulators can serve as a good osteoclast-inducing gel for biomedical applications. On similar lines, hydrogels releasing TRPV1 inhibitors can be further developed and used as ointments for the treatment of patients suffering from bone loss due to excessive osteoclast activity, as observed in the case of osteoporosis. In addition, the TRPV1 inhibitor-releasing gels can also provide pain relief by inhibiting TRPV1-mediated pain signaling. Taken together, we propose

https://doi.org/10.1021/acsomega.1c06915
ACS Omega 2022, 7, 9537−9550

that the CMT:HEMA hydrogel coated with the TRPV1 inhibitor, namely 5′-IRTX, can have biomedical applications in case of excessive bone loss due to higher osteoclast activity.

MATERIALS AND METHODS

Primary Cell Culture. All experiments involving animals were performed in accordance with guidelines of the Institutional Animal Ethics Committee (NISER/SBS/IAEC/AH-55, NISER/SBS/IAEC/AH-131, NISER/SBS/IAEC/AH-145) and the Committee for the Purpose of Control and Supervision of Experiments on Animals (CPCSEA). Male wild-type (WT) BALB/c mice (JAX stock #000651) of 4−6 weeks of age were used for isolation of primary BMMs. In brief, animals were euthanized and their femoral and tibial bone marrow was flushed out with a 5 mL syringe (Dispo Van, Hindustan Syringes and Medical Devices Ltd., 24G) and collected in RPMI 1640 complete medium (supplemented with 10% FBS, 100 U/mL penicillin/streptomycin, 1× amphotericin B). After straining it with a 70 μm cell strainer, bone marrow cells were collected, incubated with 1× RBC lysis buffer (Himedia), and seeded in 100 mm cell culture dishes (Eppendorf). Cells were grown in a humidified incubator at 37 °C, 5% CO_2.

Induction of Macrophages and Osteoclasts. After 3 days, the unadhered cell population (hematopoietic) was re-seeded in 60 mm cell culture dishes (Falcon) supplemented with 10 ng/mL MCSF (R&D Systems). Half the media was changed after 2 days. Cells were allowed to adhere for 4 days, after which the macrophages were scraped, their numbers were counted using a hemocytometer, and they were seeded on coverslips for induction to osteoclasts. 24 h post-seeding, cells were supplemented with MCSF (30 ng/mL) and RANKL (50 ng/mL; R&D Systems). After 4 days, half the media was changed and supplemented with MCSF and RANKL in the experimental set and only MCSF in the negative control set. Osteoclasts make their first appearance within 4 days and are ready for experiments by the 6th day.

Immunocytochemistry. For immunostaining, BMMs or osteoclasts were grown on 12 mm coverslips in a 24-well plate (Eppendorf). Cells were fixed with 4% paraformaldehyde (Sigma-Aldrich), followed by permeabilization with 0.1% Triton X-100 (Sigma-Aldrich) in 1X PBS for 5 min. After washing with PBS, the cells were blocked with 5% bovine serum albumin (MP Biomedicals) for 1 h at room temperature (RT). After blocking, cells were then probed with the anti-TRPV1 antibody (Rabbit host, Alomone Labs, Israel) overnight at 4 °C and detected by Alexa Fluor-488-conjugated secondary antibody (anti-rabbit, Invitrogen). DAPI (2.5 μg/mL, Invitrogen) was used to visualize nuclei. For confirming the specificity of the antibody, TRPV1 epitope-specific peptide (Alomone Labs) was used. Anti-TRPV1 antibody was pre-incubated with its blocking peptide prior to its incubation with cells. Alexa-488-labeled Phalloidin (Invitrogen) was used to label and visualize the actin cytoskeleton. Coverslips were mounted onto glass slides with Fluoromount-G (Southern Biotech). Images were taken with confocal laser-scanning microscopes Zeiss LSM 800 (60× oil immersion objective) or Olympus FV3000 (60×/1.35 NA UPlanSApo objective).

TRAP Assay. The fixative mixture (citrate, acetone, and 37% formaldehyde in 3:6:1 ratio) was prepared. The fixative solution was brought to RT(18−26 °C). Cells in each well were fixed by incubating for 3 min at RT, followed by thorough rinsing with deionized water. The TRAP solution was prepared using a TRAP kit (Sigma-Aldrich), and cells were incubated with the solution for 30 min at 37 °C. Multiple fields from each well were then imaged using the Olympus confocal microscope (FV3000) with 10× objective magnification. Images were quantified by the manual counting method using FIJI.

Coating of the CMT:HEMA Hydrogel with the TRPV1 Modulator. Carboxymethyl tamarind (CMT) polysaccharide is the derivative of tamarind gum obtained from the kernel of *Tamarindus indica*. The main advantage of tamarind seed-based polysaccharides is their easy and abundant availability. CMT possess advantages like biocompatibility, hemocompatibility, *in vitro* and *in vivo* non-toxicity, and being non-irritant[14] over the synthetic polymers, which are generally expensive, take longer time for their synthesis, and have cellular and some environmental toxicity issues.[40] It acts as an inert vehicle for the delivery of the right amount of drug and has a high drug-loading capacity,[41] which makes it a suitable candidate for the pharmaceutical industry as a drug delivery agent. TRPV1 channel modulatory drugs were mixed with CMT:HEMA gel (6 mg/mL in 1× PBS) and left to be absorbed overnight. The prepared drug−gel combination was then applied to 18 mm/25 mm coverslips, coating them evenly and left to air dry under aseptic condition. Simultaneously the coverslips were placed in 12 well/6 well culture plates. BMMs were seeded in each well (pprox.. 1×10^5 cells/well) over drug-coated coverslips and left to adhere for at least 24 h. After a sufficient number of cells had adhered to the coverslips, media supplemented with RANKL was added for experiments pertaining to osteoclasts. The media was changed with the half-depletion method after 4 days. For the TRAP assay, experiments continued for 7 days. For BMMs, cells were grown similarly as above, with the exception of the addition of RANKL.

Live Cell Imaging. BMMs were seeded on 25 mm coverslips for all live-cell experiments. Incubation with all the dyes used was done at 37 °C for the time period specified against each dye. For Ca^{2+} imaging, cells were incubated with Rhod3-AM (Thermo Fisher; 1 μM for 30 min) or Fluo4-AM (Invitrogen; 1 μM for 30 min) in complete media. Images were acquired using 40× (Rhod3-AM) or 60× (Fluo4-AM) objectives. The TRPV1 agonist/antagonist was added in the 20th frame of time-series imaging. Endogenous intracellular Ca^{2+} levels of BMMs grown on hydrogel-coated coverslips were measured using Fluo4-AM in complete media. Time-series images were acquired at a scanning rate of 100 or 200 frames for Rhod3-AM or Fluo4-AM, respectively (Olympus FV3000, 60×/1.35 NA). For assessing different subcellular parameters, the following dyes were used: H_2DCFDA (cytosolic superoxide species), DAF-FM (cytosolic NO), NAO-cardiolipin (1 μM for 30 min), JC1 (mitochondrial membrane potential), pHrodo (cytosolic pH), LysoTracker red (lysosomes), and LysoSensor green (lysosomal pH). Images were acquired using 60×/1.35 NA UPlanSApo objective (Olympus FV3000).

Quantitative Real-Time PCR (qRT-PCR). BMMs were seeded in a 6-well plate (3×10^5 cells/well). After four days of induction with MCSF and RANKL along with TRPV1 agonists and antagonists, the cells were processed for RNA extraction using an Rneasy mini kit (QIAGEN). The cDNA was synthesized using a Verso cDNA synthesis kit (Thermo Scientific). cDNA from various samples were diluted to 5 ng/μL concentration, and a total of 25 ng of DNA was used for qRT-PCR reactions, set up in a 96-well plate sealed with an optical film (Thermo Fisher). For each sample, reactions were set in triplicates. SYBR green chemistry was employed to perform

https://doi.org/10.1021/acsomega.1c06915
ACS Omega 2022, 7, 9537−9550

quantitative detection of the relative expression of mRNA levels of these genes using an ABI 7500 RT-PCR system.

Image Analysis and Statistics. Images were analyzed using ImageJ. Data were represented as mean ± SEM. Relevant statistics were performed (as mentioned in respective figure legends), and graphs were plotted using GraphPad Prism 7.

■ ASSOCIATED CONTENT

Supporting Information

The Supporting Information is available free of charge at https://pubs.acs.org/doi/10.1021/acsomega.1c06915.

> Endogenous Ca^{2+} level in BMMs upon TRPV1 activation; correlation of the area of cells and intracellular Ca^{2+}-level upon TRPV1 modulation; TRAP assay for differentiation of BMMs to osteoclasts; RT-PCR of osteoclast-specific genes; and effect of TRPV1 modulation on lysosomes (PDF)

■ AUTHOR INFORMATION

Corresponding Author

Chandan Goswami − *School of Biological Sciences, National Institute of Science Education and Research Bhubaneswar, Khurda, Odisha 752050, India; Homi Bhabha National Institute, Mumbai 400094, India;* orcid.org/0000-0002-5980-3073; Email: chandan@niser.ac.in

Authors

Ranabir Chakraborty − *School of Biological Sciences, National Institute of Science Education and Research Bhubaneswar, Khurda, Odisha 752050, India*

Tusar Kanta Acharya − *School of Biological Sciences, National Institute of Science Education and Research Bhubaneswar, Khurda, Odisha 752050, India; Homi Bhabha National Institute, Mumbai 400094, India*

Nikhil Tiwari − *School of Biological Sciences, National Institute of Science Education and Research Bhubaneswar, Khurda, Odisha 752050, India; Homi Bhabha National Institute, Mumbai 400094, India;* Present Address: Leibniz Institute for Neurobiology, Brenneckestrasse 6, Magdeburg-39120, Sachsen-Anhalt, Germany

Rakesh Kumar Majhi − *School of Biological Sciences, National Institute of Science Education and Research Bhubaneswar, Khurda, Odisha 752050, India; Homi Bhabha National Institute, Mumbai 400094, India;* Present Address: Institute for Cancer Research, Division for Cancer Medicine, Institute of Clinical Medicine, Medical Faculty, University of Oslo, Norway.

Satish Kumar − *School of Biotechnology, Kalinga Institute of Industrial Technology (KIIT), Deemed to be University, Bhubaneswar, Odisha 751024, India;* orcid.org/0000-0002-4501-1307

Luna Goswami − *School of Biotechnology, Kalinga Institute of Industrial Technology (KIIT), Deemed to be University, Bhubaneswar, Odisha 751024, India; School of Chemical Technology, Kalinga Institute of Industrial Technology (KIIT), Deemed to be University, Bhubaneswar, Odisha 751024, India;* orcid.org/0000-0002-3646-1672

Complete contact information is available at: https://pubs.acs.org/10.1021/acsomega.1c06915

Author Contributions

R.C. and T.K.A. equal contribution. Conceptualization: C.G. Manuscript writing: T.K.A., R.C., and C.G.. Data acquisition: T.K.A., R.C., N.T., S.K., and R.K.M.. Data analysis: All authors.

Notes

The authors declare no competing financial interest.

■ ACKNOWLEDGMENTS

The authors thank Indian Council of Medical Research (ICMR) for their support through IRIS Cell, ID No. 2019-1253 and RFC No. ITR/Ad-hoc/16/2019-20. The authors thank the animal house facility and imaging facility of NISER for their support. The authors also thank Dr. Saurabh Chawla for his support in animal work. Part of this work has been carried out with intramural support by DAE to C.G.

■ REFERENCES

(1) Feldman, G. L.; Weaver, D. D.; Lovrien, E. W. The Fetal Trimethadione Syndrome. *Am. J. Dis. Child.* **1977**, *131*, 1389−1392. (a) Al-Sayed, M. D.; Al-Zaidan, H.; Albakheet, A.; Hakami, H.; Kenana, R.; Al-Yafee, Y.; Al-Dosary, M.; Qari, A.; Al-Sheddi, T.; Al-Muheiza, M.; Al-Qubbaj, W.; Lakmache, Y.; Al-Hindi, H.; Ghaziuddin, M.; Colak, D.; Kaya, N. Mutations in NALCN cause an autosomal-recessive syndrome with severe hypotonia, speech impairment, and cognitive delay. *Am. J. Hum. Genet.* **2013**, *93*, 721−726. (b) Plaster, N. M.; Tawil, R.; Tristani-Firouzi, M.; Canún, S.; Bendahhou, S.; Tsunoda, A.; Donaldson, M. R.; Iannaccone, S. T.; Brunt, E.; Barohn, R.; Clark, J.; Deymeer, F.; George, A. L.; Fish, F. A.; Hahn, A.; Nitu, A.; Ozdemir, C.; Serdaroglu, P.; Subramony, S. H.; Wolfe, G.; Fu, Y.-H.; Ptáček, L. J. Mutations in Kir2.1 Cause the Developmental and Episodic Electrical Phenotypes of Andersen's Syndrome. *Cell* **2001**, *105*, 511−519. (c) Barel, O.; Shorer, Z.; Flusser, H.; Ofir, R.; Narkis, G.; Finer, G.; Shalev, H.; Nasasra, A.; Saada, A.; Birk, O. S. Mitochondrial complex III deficiency associated with a homozygous mutation in UQCRQ. *Am. J. Hum. Genet.* **2008**, *82*, 1211−1216. (d) Splawski, I.; Timothy, K. W.; Sharpe, L. M.; Decher, N.; Kumar, P.; Bloise, R.; Napolitano, C.; Schwartz, P. J.; Joseph, R. M.; Condouris, K.; Tager-Flusberg, H.; Priori, S. G.; Sanguinetti, M. C.; Keating, M. T. CaV1.2 Calcium Channel Dysfunction Causes a Multisystem Disorder Including Arrhythmia and Autism. *Cell* **2004**, *119*, 19−31.

(2) Kajiya, H. Calcium signaling in osteoclast differentiation and bone resorption. *Calcium Signal.* **2012**, *740*, 917−932.

(3) Sardar, P.; Kumar, A.; Bhandari, A.; Goswami, C. Conservation of tubulin-binding sequences in TRPV1 throughout evolution. *PLoS One* **2012**, *7*, No. e31448.

(4) Verma, P.; Kumar, A.; Goswami, C. TRPV4-mediated channelopathies. *Channels* **2010**, *4*, 319−328. (a) Nilius, B.; Voets, T. The puzzle of TRPV4 channelopathies. *EMBO Rep.* **2013**, *14*, 152−163.

(5) van der Eerden, B. C. J.; Hoenderop, J. G. J.; de Vries, T. J.; Schoenmaker, T.; Buurman, C. J.; Uitterlinden, A. G.; Pols, H. A. P.; Bindels, R. J. M.; van Leeuwen, J. P. T. M. The epithelial Ca2+ channel TRPV5 is essential for proper osteoclastic bone resorption. *Proc. Natl. Acad. Sci. U.S.A.* **2005**, *102*, 17507−17512. (a) Chamoux, E.; Bisson, M.; Payet, M. D.; Roux, S. TRPV-5 Mediates a Receptor Activator of NF-κB (RANK) Ligand-induced Increase in Cytosolic Ca2+ in Human Osteoclasts and Down-regulates Bone Resorption. *J. Biol. Chem.* **2010**, *285*, 25354−25362. (b) Van der Eerden, B. C. J.; Weissgerber, P.; Fratzl-Zelman, N.; Olausson, J.; Hoenderop, J. G. J.; Schreuders-Koedam, M.; Eijken, M.; Roschger, P.; De Vries, T. J.; Chiba, H.; Klaushofer, K.; Flockerzi, V.; Bindels, R. J. M.; Freichel, M.; van Leeuwen, J. P. T. M. The transient receptor potential channel TRPV6 is dynamically expressed in bone cells but is not crucial for bone mineralization in mice. *J. Cell. Physiol.* **2012**, *227*, 1951−1959. (c) Chen, F.; Ni, B.; Yang, Y. O.; Ye, T.; Chen, A. Knockout of TRPV6 causes osteopenia in mice by increasing osteoclastic differentiation and activity. *Cell. Physiol. Biochem.* **2014**, *33*, 796−809.

(6) Kajiya, H.; Okamoto, F.; Nemoto, T.; Kimachi, K.; Toh-Goto, K.; Nakayana, S.; Okabe, K. RANKL-induced TRPV2 expression regulates osteoclastogenesis via calcium oscillations. *Cell Calcium* **2010**, *48*, 260−269. (a) Masuyama, R.; Vriens, J.; Voets, T.; Karashima, Y.; Owsianik, G.; Vennekens, R.; Lieben, L.; Torrekens, S.; Moermans, K.; Vanden Bosch, A.; Bouillon, R.; Nilius, B.; Carmeliet, G. TRPV4-mediated calcium influx regulates terminal differentiation of osteoclasts. *Cell Metab.* **2008**, *8*, 257−265.
(7) Shuba, Y.M. Beyond neuronal heat sensing: diversity of TRPV1 heat-capsaicin receptor-channel functions. *Front. Cell. Neurosci.* **2020**, *14*, 612480.
(8) He, L.-H.; Liu, M.; He, Y.; Xiao, E.; Zhao, L.; Zhang, T.; Yang, H.-Q.; Zhang, Y. TRPV1 deletion impaired fracture healing and inhibited osteoclast and osteoblast differentiation. *Sci. Rep.* **2017**, *7*, 42385.
(9) Idris, A. I.; Landao-Bassonga, E.; Ralston, S. H. The TRPV1 ion channel antagonist capsazepine inhibits osteoclast and osteoblast differentiation in vitro and ovariectomy induced bone loss in vivo. *Bone* **2010**, *46*, 1089−1099.
(10) Shiina-Ishimi, Y.; Abe, E.; Tanaka, H.; Suda, T. Synthesis of colony-stimulating factor (CSF) and differentiation-inducing factor (D-factor) by osteoblastic cells, clone MC3T3-E1. *Biochem. Biophys. Res. Commun.* **1986**, *134*, 400−406.
(11) Rubin, J.; Fan, X.; Thornton, D.; Bryant, R.; Biskobing, D. Regulation of Murine Osteoblast Macrophage Colony-Stimulating Factor Production by 1,25(OH) 2 D 3. *Calcif. Tissue Int.* **1996**, *59*, 291−296.
(12) Helfrich, M. H. Osteoclast diseases. *Microsc. Res. Tech.* **2003**, *61*, 514−532.
(13) Sanyasi, S.; Kumar, A.; Goswami, C.; Bandyopadhyay, A.; Goswami, L. A carboxy methyl tamarind polysaccharide matrix for adhesion and growth of osteoclast-precursor cells. *Carbohydr. Polym.* **2014**, *101*, 1033−1042.
(14) Choudhury, P.; Kumar, S.; Singh, A.; Kumar, A.; Kaur, N.; Sanyasi, S.; Chawla, S.; Goswami, C.; Goswami, L. Hydroxyethyl methacrylate grafted carboxy methyl tamarind (CMT-g-HEMA) polysaccharide based matrix as a suitable scaffold for skin tissue engineering. *Carbohydr. Polym.* **2018**, *189*, 87−98.
(15) Acharya, T. K.; Kumar, S.; Tiwari, N.; Ghosh, A.; Tiwari, A.; Pal, S.; Majhi, R. K.; Kumar, A.; Das, R.; Singh, A.; Maji, P. K.; Chattopadhyay, N.; Goswami, L.; Goswami, C. TRPM8 channel inhibitor-encapsulated hydrogel as a tunable surface for bone tissue engineering. *Sci. Rep.* **2021**, *11*, 3730.
(16) Florence, A. T.; Jani, P. U. Novel oral drug formulations. *Drug Saf.* **1994**, *10*, 233−266. (a) Homayun, B.; Lin, X.; Choi, H.-J. Challenges and recent progress in oral drug delivery systems for biopharmaceuticals. *Pharmaceutics* **2019**, *11*, 129.
(17) Li, J.; Mooney, D. J. Designing hydrogels for controlled drug delivery. *Nat. Rev. Mater.* **2016**, *1*, 16071. (a) Tibbitt, M. W.; Dahlman, J. E.; Langer, R. Emerging frontiers in drug delivery. *J. Am. Chem. Soc.* **2016**, *138*, 704−717.
(18) Domazetovic, V.; Marcucci, G.; Iantomasi, T.; Brandi, M. L.; Vincenzini, M. T. Oxidative stress in bone remodeling: role of antioxidants. *Clin. Cases Miner. Bone Metab.* **2017**, *14*, 209.
(19) Agidigbi, T. S.; Kim, C. Reactive oxygen species in osteoclast differentiation and possible pharmaceutical targets of ROS-mediated osteoclast diseases. *Int. J. Mol. Sci.* **2019**, *20*, 3576.
(20) Auten, R. L.; Davis, J. M. Oxygen toxicity and reactive oxygen species: the devil is in the details. *Pediatr. Res.* **2009**, *66*, 121−127.
(21) Brandi, M. L.; Hukkanen, M.; Umeda, T.; Moradi-Bidhendi, N.; Bianchi, S.; Gross, S. S.; Polak, J. M.; MacIntyre, I. Bidirectional regulation of osteoclast function by nitric oxide synthase isoforms. *Proc. Natl. Acad. Sci. U.S.A.* **1995**, *92*, 2954−2958.
(22) Boyle, W. J.; Simonet, W. S.; Lacey, D. L. Osteoclast differentiation and activation. *Nature* **2003**, *423*, 337−342.
(23) Pederson, L.; Ruan, M.; Westendorf, J. J.; Khosla, S.; Oursler, M. J. Regulation of bone formation by osteoclasts involves Wnt/BMP signaling and the chemokine sphingosine-1-phosphate. *Proc. Natl. Acad. Sci. U.S.A.* **2008**, *105*, 20764−20769.
(24) Asagiri, M.; Takayanagi, H. The molecular understanding of osteoclast differentiation. *Bone* **2007**, *40*, 251−264.
(25) Wilson, S. R.; Peters, C.; Saftig, P.; Brömme, D. Cathepsin K activity-dependent regulation of osteoclast actin ring formation and bone resorption. *J. Biol. Chem.* **2009**, *284*, 2584−2592.
(26) Ebeling, P. R.; Nguyen, H. H.; Aleksova, J.; Vincent, A. J.; Wong, P.; Milat, F. Secondary Osteoporosis. *Endocr. Rev.* **2021**, DOI: 10.1210/endrev/bnab028.
(27) Nishimura, H.; Kawasaki, M.; Tsukamoto, M.; Menuki, K.; Suzuki, H.; Matsuura, T.; Baba, K.; Motojima, Y.; Fujitani, T.; Ohnishi, H.; Yamanaka, Y.; Kosugi, K.; Okada, Y.; Tokuda, K.; Tajima, T.; Yoshioka, T.; Okimoto, N.; Ueta, Y.; Sakai, A. Transient receptor potential vanilloid 1 and 4 double knockout leads to increased bone mass in mice. *Bone Rep.* **2020**, *12*, 100268.
(28) Reni, C.; Mangialardi, G.; Meloni, M.; Madeddu, P. Diabetes stimulates osteoclastogenesis by acidosis-induced activation of transient receptor potential cation channels. *Sci. Rep.* **2016**, *6*, 30639.
(29) Khan, K.; Singh, A.; Mittal, M.; Sharan, K.; Singh, N.; Dixit, P.; Sanyal, S.; Maurya, R.; Chattopadhyay, N. [6]-Gingerol induces bone loss in ovary intact adult mice and augments osteoclast function via the transient receptor potential vanilloid 1 channel. *Mol. Nutr. Food Res.* **2012**, *56*, 1860−1873.
(30) Callaway, D. A.; Jiang, J. X. Reactive oxygen species and oxidative stress in osteoclastogenesis, skeletal aging and bone diseases. *J. Bone Miner. Metab.* **2015**, *33*, 359−370.
(31) Collin-Osdoby, P.; Rothe, L.; Bekker, S.; Anderson, F.; Osdoby, P. Decreased nitric oxide levels stimulate osteoclastogenesis and bone resorption both in vitro and in vivo on the chick chorioallantoic membrane in association with neoangiogenesis. *J. Bone Miner. Res.* **2000**, *15*, 474−488. (a) Zheng, H.; Yu, X.; Collin-Osdoby, P.; Osdoby, P. RANKL Stimulates Inducible Nitric-oxide Synthase Expression and Nitric Oxide Production in Developing Osteoclasts. *J. Biol. Chem.* **2006**, *281*, 15809−15820.
(32) Lemma, S.; Sboarina, M.; Porporato, P. E.; Zini, N.; Sonveaux, P.; Di Pompo, G.; Baldini, N.; Avnet, S. Energy metabolism in osteoclast formation and activity. *Int. J. Biochem. Cell Biol.* **2016**, *79*, 168−180.
(33) Ursu, D.; Knopp, K.; Beattie, R. E.; Liu, B.; Sher, E. Pungency of TRPV1 agonists is directly correlated with kinetics of receptor activation and lipophilicity. *Eur. J. Pharmacol.* **2010**, *641*, 114−122.
(34) Kumar, A.; Majhi, R. K.; Acharya, T. K.; Smalla, K.-H.; Gundelfinger, E. D.; Goswami, C. TRPV4 interacts with mitochondrial proteins and acts as a mitochondrial structure-function regulator. bioRxiv: 330993, **2018**. (a) Yadav, M.; Goswami, C. TRPV3 mutants causing Olmsted Syndrome induce impaired cell adhesion and nonfunctional lysosomes. *Channels* **2017**, *11*, 196−208.
(35) Lacombe, J.; Karsenty, G.; Ferron, M. Regulation of lysosome biogenesis and functions in osteoclasts. *Cell Cycle* **2013**, *12*, 2744−2752.
(36) Križaj, D.; Mercer, A. J.; Thoreson, W. B.; Barabas, P. Intracellular pH modulates inner segment calcium homeostasis in vertebrate photoreceptors. *Am. J. Physiol.: Cell Physiol.* **2011**, *300*, C187−C197.
(37) Trapp, S.; Lâkermann, M.; Kaila, K.; Ballanyi, K. Acidosis of hippocampal neurones mediated by a plasmalemmal Ca2+/H+ pump. *Neuroreport* **1996**, *7*, 2000−2004.
(38) Swallow, C. J.; Grinstein, S.; Rotstein, O. D. Cytoplasmic pH regulation in macrophages by an ATP-dependent and N,N′-dicyclohexylcarbodiimide-sensitive mechanism. Possible involvement of a plasma membrane proton pump. *J. Biol. Chem.* **1988**, *263*, 19558−19563.
(39) Thomas, K. C.; Sabnis, A. S.; Johansen, M. E.; Lanza, D. L.; Moos, P. J.; Yost, G. S.; Reilly, C. A. Transient receptor potential vanilloid 1 agonists cause endoplasmic reticulum stress and cell death in human lung cells. *J. Pharmacol. Exp. Ther.* **2007**, *321*, 830−838.
(40) Avachat, A. M.; Dash, R. R.; Shrotriya, S. N. Recent investigations of plant based natural gums, mucilages and resins in novel drug delivery systems. *Indian J. Pharm. Educ. Res.* **2011**, *45*, 86−99.

https://doi.org/10.1021/acsomega.1c06915
ACS Omega 2022, 7, 9537−9550

(41) Kulkarni, D.; Dwivedi, A.; Sarin, J. S.; Singh, S. Tamarind seed polyose: A potential polysaccharide for sustained release of verapamil hydrochloride as a model drug. *Indian J. Pharm. Sci.* **1997**, *59*, 1.

https://doi.org/10.1021/acsomega.1c06915
ACS Omega 2022, 7, 9537−9550